Clinical Infectious Diseases

SUPPLEMENT ARTICLE

Perinatally Human Immunodeficiency Virus–Infected Adolescents and Young Adults Demonstrate Distinct BNT162b2 Messenger RNA Coronavirus Disease 2019 Vaccine Immunogenicity

Elena Morrocchi,[1,2,a] Chiara Pighi,[1,a] Giuseppe Rubens Pascucci,[1,3] Nicola Cotugno,[1,4] Chiara Medri,[1] Donato Amodio,[1] Luna Colagrossi,[5] Alessandra Ruggiero,[1] Emma Concetta Manno,[1] Chiara Casamento Tumeo,[6] Stefania Bernardi,[1] Kinga K. Smolen,[2,7] Carlo Federico Perno,[5] Al Ozonoff,[2,7] Paolo Rossi,[1] Ofer Levy,[2,7,8] and Paolo Palma[1,2,4]

[1]Academic Department of Pediatrics, Research Unit of Clinical Immunology and Vaccinology, Bambino Gesù Children's Hospital, Rome, Italy; [2]Precision Vaccines Program, Boston Children's Hospital, Boston, Massachusetts, USA; [3]Department of Systems Medicine, University of Rome "Tor Vergata," Rome, Italy; [4]Department of Systems Medicine, University of Rome "Tor Vergata," Rome, Italy; [5]Department of Microbiology, Bambino Gesù Children's Hospital, Rome, Italy; [6]General Pediatrics Unit, Department of Emergency, Acceptance and General Pediatrics, Bambino Gesù Children's Hospital, Rome, Italy; [7]Harvard Medical School, Boston, Massachusetts, USA; and [8]Broad Institute of Massachusetts Institute of Technology and Harvard, Cambridge, Massachusetts, USA

Background. Immunization of vulnerable populations with distinct immunity often results in suboptimal immunogenicity, durability, and efficacy.

Methods. Safety and immunogenicity profiles of BNT162b2 messenger RNA coronavirus disease 2019 (COVID-19) vaccine, among people living with human immunodeficiency virus (HIV), were evaluated in 28 perinatally HIV-infected patients under antiretroviral therapy (ART) and 65 healthy controls (HCs) with no previous history of COVID-19. Thus, we measured severe acute respiratory syndrome coronavirus 2 (SARS-CoV-2)–specific humoral and CD4+ T cell responses. Samples were collected before vaccination (baseline, day [D] 0), at the second dose (D21), and at 4 weeks (D28) and 6 months (D180) after D0. Proteomic profiles at D0 and D28 were assessed with a multiplexed proximity extension assay (Olink) on plasma samples.

Results. All HIV-infected patients mounted similar anti–SARS-CoV-2 humoral responses to those of HCs, albeit with lower titers of anti-trimeric S at D28 ($P = .01$). Only peripheral blood mononuclear cells of HIV-infected patients demonstrated at D28 an impaired ability to expand their specific (CD40L+) CD4+ T-cell populations. Similar humoral titers were maintained between the 2 groups at 6-months follow-up. We additionally correlated baseline protein levels to either humoral or cellular responses, identifying clusters of molecules involved in immune response regulation with inverse profiles between the 2 study groups.

Conclusions. Responses of ART-treated HIV-infected patients, compared to those of HCs, were characterized by distinct features especially within the proteomic compartment, supporting their eligibility to an additional dose, similarly to the HC schedule.

Keywords. BNT162b2 mRNA COVID-19 vaccine; SARS-CoV-2 antibody; COVID-19; perinatally HIV-infected patients; antigen-specific T cells.

The most recent G7 summit in June 2021 highlighted a strategy to end the coronavirus disease 2019 (COVID-19) pandemic by immunizing 70% of the world's population by mid-2022. So far, even if the 58% of the worldwide community has received at least 1 dose (data updated to mid-December), to limit the next COVID-19 infection wave, the Italian Ministry of Health started by mid-September the administration of booster doses for at-risk members of the population. Despite some initial evidence to the contrary, recent studies suggest that human immunodeficiency virus (HIV) type 1 infection increases the risk of severe COVID-19 [1–3], thus highlighting the need for an efficient vaccination schedule for people living with HIV (PLWH) [4]. This strategy is also meant to prevent lack of access to antiretroviral therapy (ART) for this vulnerable population, as already seen at the beginning of the COVID-19 pandemic increasing the possible worsening of their health condition [5].

Studies of healthy adults demonstrate how BNT162b2 messenger RNA (mRNA) vaccine generally induces robust

[a]E. M. and C. P. contributed equally to this work.

Correspondence: P. Palma, Clinical and Research Unit of Clinical Immunology and Vaccinology, Academic Department of Pediatrics, IRCCS Bambino Gesù Children's Hospital, Piazza S. Onofrio, Rome, Italy 4-00165 (paolo.palma@opbg.net).

Clinical Infectious Diseases® 2022;75(S1):S51–60

https://doi.org/10.1093/cid/ciac408

and protective humoral and cellular responses to the severe acute respiratory syndrome coronavirus 2 (SARS-CoV-2) spike (S) protein [6] and provides protection from severe infection with SARS-CoV-2 [7]. In contrast, individuals with impaired immunity may experience reduced BNT162b2 mRNA vaccine–induced protection, as recently investigated by our group [8, 9]. In general, PLWH often show suboptimal immune responses to a range of vaccines, that even though improve with ART, often remain lower or decline more easily than in HIV-negative or healthy control (HC) subjects [10–13]. Although the safety and efficacy of the Pfizer-BNT162b2 mRNA vaccine has already been tested in a multinational trial of >40 000 participants [7], to our knowledge data in this study regarding the 196 HIV-positive (HIV^+) individuals included in the cohort have yet to be published. More recently, a few short-term follow-up studies have reported good tolerability and BNT162b2 humoral immunogenicity (antibody [Ab] responses) in ART-adherent HIV^+ subjects [4, 13–15], with the exception of 1 patient with uncontrolled HIV infection and a low $CD4^+$ T-cell count [16]. Although few data are thus far available on vaccine-induced cellular responses as well as on maintenance over time of SARS-CoV-2–specific humoral responses in HIV^+ patients, conversely to HCs [17], an early boosting has been suggested in many countries.

With this purpose, we assessed safety and immunogenicity in relation to the plasma proteome profiles over 6 months of BNT162b2 vaccine in ART-treated perinatally HIV-infected adolescents and young adults enrolled at Bambino Gesù Children Hospital in Rome.

Table 1. Study Cohort Characteristics

Characteristic	HIV-Positive Participants (N = 28)
Female sex, No. (%)	14 (50)
Age, y, mean ± SD	24.7 ± 5.4
Race/ethnicity, No.	
White	11
Black/African	12
Hispanic/Latino	3
Other/unknown	2
ART initiation, No. (%)	
Early treated: <6 mo	11 (39.3)
Late treated: >6 mo	17 (60.7)
ART therapy (drug class), No. of patients	
INI+ NRTI	7
INI + PI	7
INI + 2 NRTIs	7
2 NRTIs + PI	2
NRTI + PI	1
INI + NNRTI	1
PI + NNRTI	1
PI + NNRTI + INI	1
2 NRTIs + PI + INI	1
ART duration, y, mean (IQR)	17.4 (9–28)
Viral load <40 copies/mL, No. (%)	25 (89.3)
WBCs/mL, mean ± SD	5885 ± 1652
Lymphocytes, cells/mL, mean ± SD	2050 ± 877.8
CD3%	75.9 ± 9.0
CD4%	31.8 ± 7.7
CD8%	37.5 ± 8.9
CD19%	12.1 ± 4.2
$CD16^+CD56^+$%	10.8 ± 7.1
$CD4^+/CD8^+$ ratio	0.90 ± 0.35

Abbreviations: ART, antiretroviral therapy; HIV, human immunodeficiency virus; INI, integrase inhibitor; IQR, interquartile range; NNRTI, nonnucleoside reverse transcriptase inhibitor; NRTI, nucleoside reverse transcriptase inhibitor; PI, protease inhibitor; SD, standard deviation; WBC, white blood cells.

METHODS

Study Participants and Study Design

Twenty-eight ART-treated perinatally HIV-infected young adults were enrolled from 10 to 25 March 2021 at Bambino Gesù Children's Hospital in Rome, Italy. Characteristics of the HIV cohort are shown in Table 1. Per national regulations, only residents in the Latium region were eligible for vaccination in our center. This observational study included HIV^+ patients aged 18–35 years, of whom 50% were female, who received BNT162b2 mRNA COVID-19 vaccine, with a schedule of 2 doses of 30 μg 21 days apart [18]. Longitudinal samples were collected the day of the first dose (D0) at the second dose(D21), 4 weeks (D28), and 6 months (D180) after the first dose (Figure 1*A*). Serology and molecular (nasopharyngeal swabs) tests for SARS-CoV-2 were performed prior to vaccination. All patients were negative for SARS-CoV-2 Abs, both anti-spike (S) and anti-nucleocapsid (N) proteins, at D0. Sixty-five HCs aged <60 years (70.8% of females), with no comorbidities who received BNT162b2 mRNA COVID-19 vaccine were used as a control group. All participants received a survey where they reported any adverse events and side effects following each dose of vaccine. In accordance with national regulations, the study protocol was communicated to the Ethical Committee of the National Infectious Disease Center at Spallanzani Institute (acceptance number 462) and accepted by the local ethical committee (CONVERS STUDY: "Evaluation of COvid-19 mRNA BNT162b2 (Comirnaty) VaccinE immunogenicity in vulneRable populationS"; protocol number 409_OPBG_2021). Written informed consent was obtained from all participants or legal guardians.

Sample Collection and Storage

Venous blood was collected in ethylenediaminetetraacetic acid tubes and processed within 2 hours. Plasma isolated from blood was stored at −80°C. Peripheral blood mononuclear cells (PBMCs) were isolated from blood with Ficoll density gradient and cryopreserved in fetal bovine serum with 10% dimethyl sulfoxide until analysis, in liquid nitrogen.

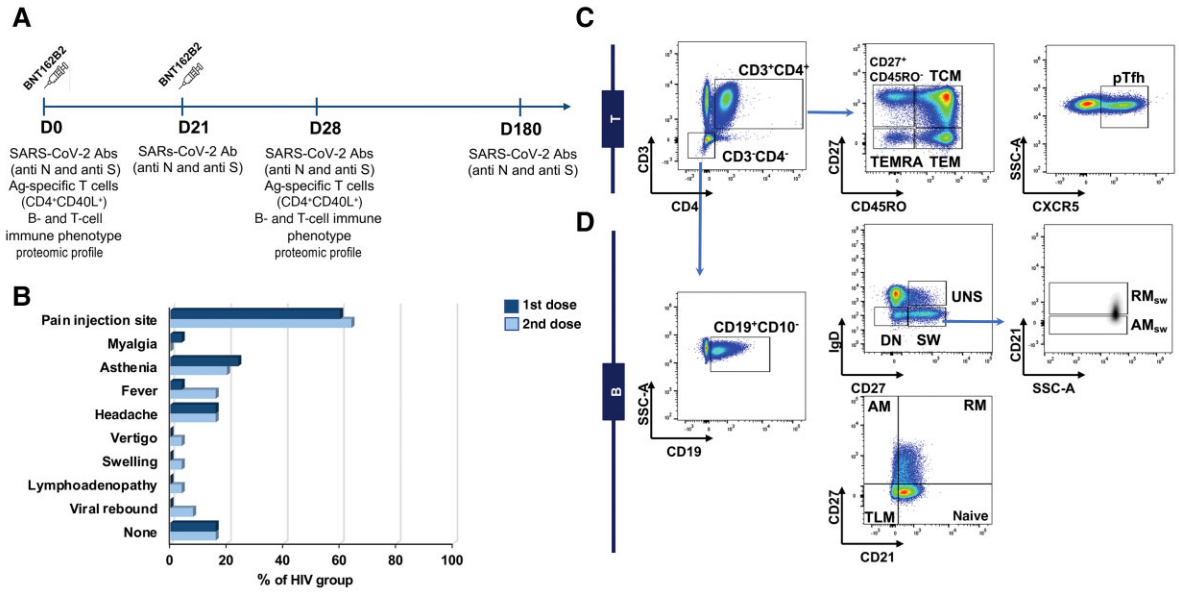

Figure 1. Study design and safety profile of BNT162b2 messenger RNA (mRNA) coronavirus disease 2019 (COVID-19) vaccine. *A*, Study design. *B*, Adverse events after the first and second doses of BTN162b2 mRNA COVID-19 vaccine in the human immunodeficiency virus–infected study group. *C* and *D*, Representative gating strategies for $CD3^+CD4^+$ T-cell (*C*) and B-cell (*D*) subsets. Abbreviations: Ab, antibody; Ag, antigen; AM, activated memory B cells; DN, double negative B cells ; HIV, human immunodeficiency virus; IgD, immunoglobulin D; TLM, tissue-like memory B cells; pTfh, peripheral T follicular helper cells; RM, resting memory B cells; SARS-CoV-2, severe acute respiratory syndrome coronavirus 2; SSC-A, side scatter area; SW, switched memory B cells; TCM, central memory T cells; TEM, effector memory T cells; TEMRA, terminally differentiated effector memory T cells; UNS, unswitched memory B cells.

Humoral Response

Anti–SARS-CoV-2 immunoglobulin G (IgG) Ab titers were measured as previously described [8, 19] at D0, D21, D28, and D180. For this purpose, to expand the range of antibodies detected, 2 different assays were employed: the LIAISON SARS-CoV-2 TrimericS-IgG and the Elecsys Anti-SARS-CoV-2 S assays, performed on automated analyzers following the manufacturer's instructions. Additional information are listed in the Supplementary Materials.

Antigen-Specific $CD4^+$ T Cells by Flow Cytometry

SARS-CoV-2–specific $CD4^+CD40L^+$ T cells were identified as previously described [9]. In brief, thawed PBMCs were plated (1.5×10^6/aliquot/200 µL) in 96-well plates containing CD154-PE (CD40L, BD PharMingen, Franklin Lakes, New Jersey), anti-CD28 (1 mg/mL) and 0.4 mg/mL PepTivator SARS-CoV-2 Prot_S (Miltenyi Biotec, Bergisch Gladbach, Germany), or medium only. Following a 16-hour incubation at 37°C/5% carbon dioxide, PBMCs were centrifuged and stained with LIVE/DEAD fixable NEAR-IR dead cell stain kit (ThermoFisher, Waltham, Massachusetts) 1 µL/10^6 cells/mL for 15 minutes at room temperature, protected by light. Surface staining was performed as listed in the Supplementary Materials. T- and B-cell populations (Figure 1*C* and 1*D*) and SARS-CoV-2–specific ($CD40L^+$) $CD4^+$ T cells were gated as previously reported [8, 9]. Delta-delta (ΔΔ) values used for correlation analyses were calculated, for each population, by subtracting the frequency differences between stimulated and unstimulated samples collected at D28 (ΔD28) and D0 (ΔD0).

Olink Assay

Plasma samples were randomized and analyzed for immune-related protein biomarkers through a multiplexed proximity extension assay as previously described [20] before (D0) and 4 weeks (D28) after the first dose of BTN162b2 vaccination. Proteomic analyses employed the Inflammation and Immune Response Olink kits [21]. Data are reported in arbitrary units as normalized protein expression (NPX) that enables individual protein analysis across a sample set analyzed in $\log_2$ scale, wherein a higher NPX correlates with higher protein expression. The data were preprocessed using the NPX Manager Software and OlinkAnalyze R package (version 1.3.0). NPX values below the limit of detection (LOD) were replaced with LOD values.

Statistical Analysis

Statistical analyses were performed using GraphPad Prism 8 (GraphPad, San Diego, California) and R (version 4.1.1) software. Proteins with an interquartile range (IQR) value <20th percentile of the IQR value distribution were excluded from further analysis. D'Agostino-Pearson or Shapiro tests were used to assess data distribution, and statistical comparisons with *t* test were performed with normally distributed data or

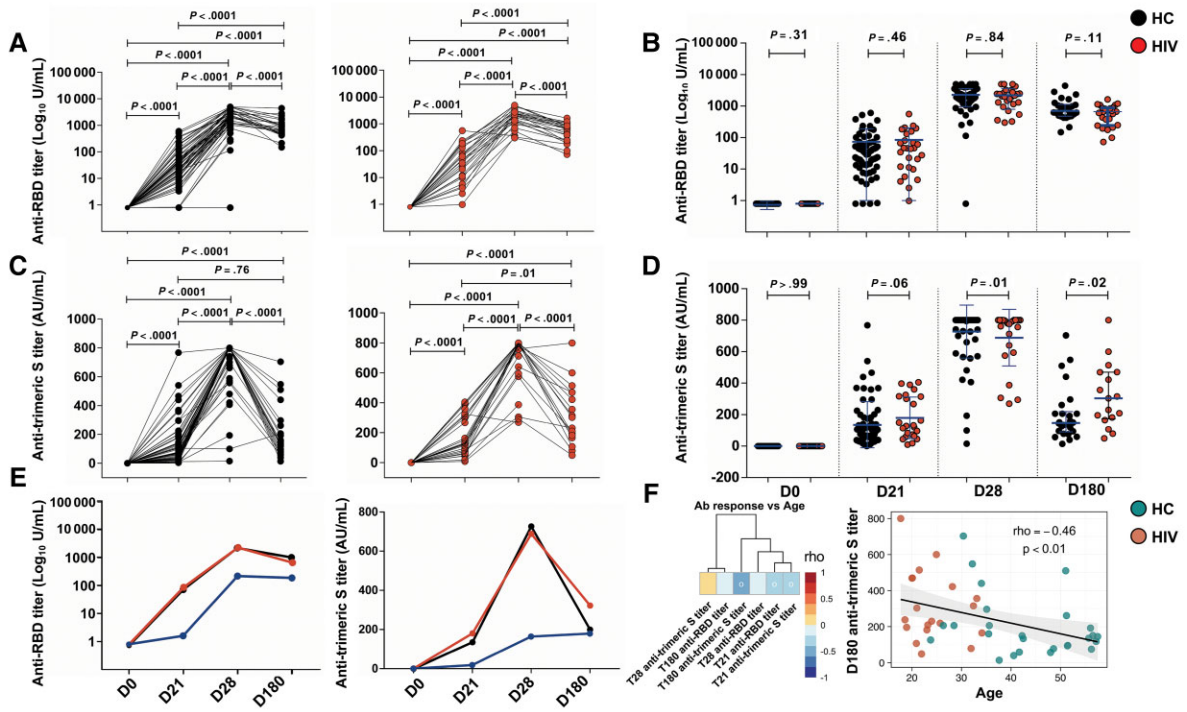

Figure 2. Both human immunodeficiency virus (HIV)–infected individuals and healthy controls (HCs) demonstrate robust BTN162b2 messenger RNA (mRNA) coronavirus disease 2019 (COVID-19)–vaccine-induced anti–severe acute respiratory syndrome coronavirus 2 (SARS-CoV-2) humoral response exceeding that of solid organ transplant recipients (Tx). Humoral response was evaluated before (D0) and 21 days (D21), 4 weeks (D28), and 6 months (D180) after the first dose of BTN162b2 mRNA COVID-19 vaccine as anti-S1 receptor binding domain (RBD) (*A* and *B*) and anti-trimeric S (*C* and *D*) antibody (Ab) titers. Anti-RBD and anti-trimeric S Abs were assessed by Elecsys Anti-SARS-CoV-2 S assay (Roche, lower cutoff 0.8 U/mL, higher cutoff 800 U/mL) and LIAISON 166 SARS-CoV-2 TrimericS–immunoglobulin G assay (Diasorin, cutoff 13 AU/mL) in the HIV (red dots: n = 27, anti-RBD; n = 25, anti-trimeric S) and HC (black dots: n = 65) study groups, respectively. Scatterplot graphs depict mean ± standard deviation. *E*, Plot depicts Ab titer mean values in HCs (black lines: n = 65), HIV (red lines: n = 27, anti-RBD; n = 25, anti-trimeric S), and Tx (blue lines: n = 29). Differences in Ab load at D21, D28, and D180 between Tx and HIV or HC groups were all significant, except for anti-trimeric S levels in Tx vs HCs at D180 ($P = .10$). Wilcoxon signed-rank test and Mann-Whitney test were used to assess differences in the Ab load between the time points and between HC, HIV, and Tx groups, respectively. Significance was set at $P < .05$. *F*, Heatmap plot showing Spearman correlations between age and anti-RBD or anti-trimeric S Ab titers at D21, D28, and D180. Red indicates positive correlations and blue negative ones. The colored scale ranging from 1 and −1 indicates the ρ values. Dots highlight significant correlations with adjusted $P < .05$ (left panel). Spearman correlation between age and anti-trimeric S titer at D180 in both the HIV (red dots) and HC (green dots) groups, with ρ and *P* defining the statistical significance (right panel).

with the nonparametric paired (Wilcoxon) and unpaired (Mann-Whitney) tests. Spearman correlation was used to examine the association between variables/features. All tests were 2-tailed and statistical significance was set at $P < .05$. For multiple comparison tests, the *P* values were adjusted according to the false discovery rate method. In correlation heatmaps, only the proteins with an opposite trend (ρ mean value >0.2 or <−0.2) in the HIV$^+$ and HC groups were shown. The R package enrichR v3.0 [22] was used to perform pathway enrichment analysis in GO Biological Process 2021 databases.

RESULTS

Study Participants

The study cohort included 28 HIV$^+$ young adults between 18 and 35 years of age (mean age, 24.7 ± 5.4 standard deviation [SD]), followed at Bambino Gesù Children Hospital in Rome, and 65 vaccinated HCs aged 24–59 years (mean age, 45.1 ± 9.5 SD) served as the control group. All HIV patients were treated with ART (mean treatment duration, 17.4 years) and virally suppressed at the time of immunization, except for 3 participants (10.7%). They demonstrated a viremia of 174 copies/mL, 769 copies/mL, and 2831 copies/mL at the time of vaccination (D0) and for the first 2 participants became undetectable at D28, whereas 416 copies/mL was detected for the last participant. Clinical and laboratory data for this cohort are provided in Table 1.

Safety Profile of BNT162B2 mRNA COVID-19 Vaccine

Questionnaires administered after the first and second doses reported that BNT162b2 vaccine was well tolerated, with adverse events (AEs) largely mirroring those reported in other study populations and with no hospitalization needed (Figure 1*B*). We also noticed that among our HIV$^+$ cohort, 2 of 28 study participants demonstrated a viral load (VL) >40 copies/mL at D28 despite being undetectable at D0, but follow-up visits

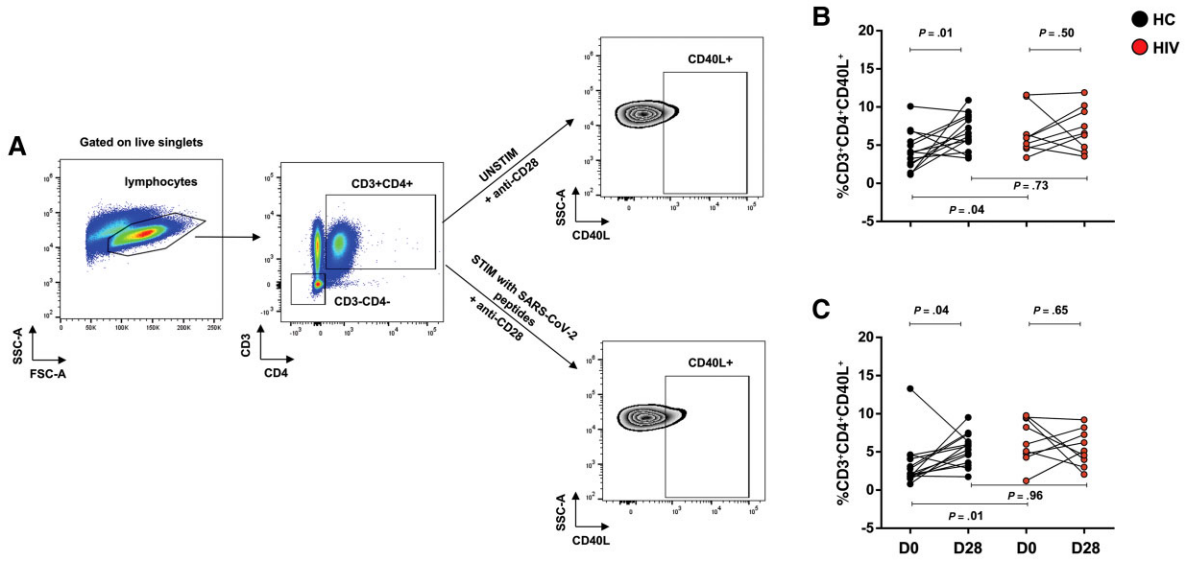

Figure 3. Severe acute respiratory syndrome coronavirus 2 (SARS-CoV-2)–specific $CD4^+$ T-cell response before (D0) and 4 weeks after the first dose (D28) of SARS-CoV-2 messenger RNA BTN162b2 vaccination. *A*, Representative gating strategy for SARS-CoV-2–specific $CD3^+CD4^+$ T cells after 16 hours' in vitro stimulation with SARS-CoV-2 peptides. Frequencies of antigen-specific ($CD40L^+$) $CD3^+CD4^+$ T cells at D0 and D28 are shown for both the HIV (red dots: n = 9) and healthy control (HC) (black dots: n = 14) study groups in the absence (*B*) or presence (*C*) of 16 hours' in vitro stimulation with SARS-CoV-2 peptides. Wilcoxon signed-rank test and Mann-Whitney test were used to assess differences in cell frequencies between the time points and between the HC and HIV groups, respectively. Abbreviations: FSC-A forward scatter area; HC, healthy control; HIV, human immunodeficiency virus; SARS-CoV-2, severe acute respiratory syndrome coronavirus 2; SSC-A, side scatter area; STIM, stimulated; UNSTIM, unstimulated.

determined that these bouts of viremia were short-lived blips as after 6 months all values returned to <40 copies/mL.

Anti-SARS-CoV-2 Ab Responses in HIV^+ and HC Cohorts

Results summarized in Figure 2A and 2C show the overall ability for both HC and HIV groups to significantly ($P < .0001$) increase anti–SARS-CoV-2 Ab titers between D21 and D28. At D21 both anti–receptor-binding domain (RBD) (Figure 2*B*) and anti-trimeric S (Figure 2*D*) Ab levels were similar in the 2 study groups, whereas the HIV group demonstrated a lower median increase in anti-trimeric S Abs at D28 compared to HCs ($P = .01$; Figure 2*D*). It is also important to report that while 1 HC subject lacked anti-RBD Ab titer at the end of the vaccination schedule, all the HIV patients had detectable SARS-CoV-2 IgG Abs at D28. A significant reduction ($P < .0001$) of 2.2- and 3.5- fold in anti-RBD Ab levels were found in the HC and HIV groups, respectively, at D180 compared to D28 (Figure 2*A*), but no significant difference was present in D180 Ab levels between the 2 study groups (Figure 2*B*). A diverse fate was followed by Abs recognizing different epitopes of SARS-CoV-2 spike (S) protein in its trimeric form or native conformation (anti-trimeric S). A significant reduction ($P < .0001$) was observed at D180 in both study groups (Figure 2*C*), but still 1.6-fold higher anti-trimeric S levels were measured in HIV^+ when compared to HCs ($P = .02$, Figure 2*D*). Overall, these results on the humoral response of HIV^+ compared to HCs, render them divergent from another model of secondary immunocompromise represented by solid organ transplant recipients (Tx) (Figure 2*E*). Differences in Ab load at D21, D28, and D180 between Tx and the HIV or HC groups were all significant, except for anti-trimeric S levels in Tx vs HCs at D180 ($P = .10$).

When we evaluated the possible role of age within Ab data, we found that it was negatively correlated with anti-trimeric S titers at D180 (Figure 2*F*). Thus, to evaluate whether HIV^+ subjects, well known for exhibiting precocious immunosenescence, demonstrate similar characteristics to elderly HCs, we conducted the same analysis by dividing HCs into younger (age ≤55 years) and older (age >55 years) subgroups. At the same time, to verify the effect of ART initiation time, previously shown to positively impact on the development and maintenance of immunity toward routine vaccines, we further stratified the HIV group into early treated (ET) and late treated (LT). Compared to younger HCs (Supplementary Figure 1*B*), HIV^+ ($P < .01$) and, more specifically, both ET ($P = .02$) and LT ($P = .01$) patients exhibited at D28 significantly lower anti-trimeric S levels, which increased to comparable levels in the long-term. On the other hand, when compared to older HCs (Supplementary Figure 1*D*), HIV^+ showed comparable anti-trimeric S levels at D28 ($P = .59$), reaching even higher levels at T180 ($P = .02$). These results were confirmed when anti-trimeric S levels at D28 and D180 in ET were compared to older HCs ($P = .62$ and $P = .03$; Supplementary Figure 1*D*). Conversely, older HCs and LT patients exhibited, at both

time points, comparable anti-trimeric S levels ($P = .65$ and $P = .05$, Supplementary Figure 1*D*).

Cellular Response

To characterize cellular SARS-CoV-2 mRNA vaccine immunogenicity, we assessed the frequency of SARS-CoV-2–specific $CD4^+CD40L^+$ T cells after in vitro stimulation of PBMCs with SARS-CoV-2 peptides (representative gate in Figure 3*A*) as previously described [21]. We evaluated the antigen (Ag)–specific cellular response at D0 and D28 in both the HIV (n = 9) and HC (n = 14) groups observing an overall statistically significant expansion of the $CD4^+CD40L^+$ T cells only in HCs (Figure 3*B* and 3*C*). In addition, a considerable increase in central memory T (TCM) $CXCR5^+CD40L^+$ cells, also known as peripheral T-follicular helper (pTfh)/$CD40L^+$ cells, was found only in HCs with or without SARS-CoV-2 peptide in vitro stimulation ($P < .01$, Figure 4*C*). Of note, no major changes within circulating $CD4^+$ T-cell subsets (representative gate in Figure 1*C*), which could explain such lack in Ag-specific cell expansion, were found in the HIV group between D0 and D28 (data not shown). Similarly, no major differences were observed in phenotypic maturation profile among B-cell subsets (representative gate in Figure 1*D*) upon vaccination (data not shown). Thus, to assess whether differences within the distribution of $CD4^+$ T-cell subsets might contribute to the inability of HIV individuals to expand Ag-specific $CD4^+$ T cells at the end of vaccination schedule, cell frequencies at D0 and D28 were evaluated in both study groups. We noted comparable proportions of total $CD3^+CD4^+$ (Figure 4*A*) and $CD4^+$ T-cell subpopulations (Figure 4*B*).

Distinct Plasma Proteomic Profiles Between Vaccinated HIV^+ and HC Subjects

To examine the study cohort's plasma proteome, the Olink platform was used to measure 180 different proteins in each study participant, before (D0) and after (D28) vaccination. To avoid the potential confounding factor of age, proteins negatively or positively correlating with this variable were excluded from the analysis (n = 45) (Supplementary Figure 2*A*). Principal component analysis on baseline samples depicted in Figure 5*A* demonstrated 2 clear clusters that persist when age-matched cohorts are considered (Supplementary Figure 2*B*). These observations imply that the HIV infection leads to a clearly identifiable distinct plasma proteome. For the pathway enrichment analysis, we considered only the top 20 PC2 loading molecules (Figure 5*B*) mostly contributing to the clustering, while the top 20 PC1 molecules are listed in Supplementary Figure 2*C*. Analysis revealed modulators of T cell receptor signaling and T-cell activation (SH2D1A and SH2B3) and proteins related to SARS-CoV-2 innate immune evasion and cell-specific immune response (TANK and DDX58), as well as novel intracellular components of the RIG-I–like receptor (RLR) pathway (TANK and DDX58) (all adjusted $P = .02$). Host helicase RLRs recognize viral pathogen RNA and initiate signaling pathways triggering the innate antiviral response via production of type I interferons and inflammatory cytokines. Interestingly, when we performed a proteomic differential analysis between D0 and D28, we found only 6 differentially produced proteins in HIV patients (all adjusted $P < .05$), either up-regulated (MASP1) or down-regulated (ITM2A, LILRB4, SH2B3, STC1, and TANK) at D28 (Supplementary Figure 2*D*). Conversely, no significant differences between D0 and D28 were found in the plasma proteome of the HC group, suggesting that BNT162b2 mRNA vaccine does not induce stable modification at a proteomic level 7 days after the booster dose (D28).

Correlations of Baseline Proteomic Profiles With Anti–SARS-CoV-2–Specific Humoral and $CD4^+$ T-Cell Responses

To verify whether the baseline expression of plasma proteins related to immune response and inflammation predicts mRNA vaccine immunogenicity, we performed correlation analyses of proteomic data at D0 with anti-RBD and anti-trimeric S Ab levels at D21, D28, or D180 in both study groups. Figure 5*C* depicts an unsupervised heatmap showing a Spearman correlation matrix of 11 proteins, which were clearly correlated in opposite ways with the humoral response of the 2 groups. Within this cluster, the enrichment analysis (Figure 5*D*) revealed 4 proteins (AREG, IL-10, IL12RB1, and IFNLR1) that are part of pathways involved in cytokine responses, positive regulation of cytokine production, regulation of cell proliferation, and IL-12 signaling pathways. Of note, HIV^+ maintained only negative correlations with these molecules, highlighting the need to have lower basal levels of inflammatory molecules to be able to mount a specific humoral response compared to HCs. Another interesting molecule is CD83, pivotal in Ag presentation and lymphocyte activation, which was still negatively correlated only in HIV^+ (Figure 5*C*). The same strategy described above was also followed to correlate proteomic data at D0 and ΔΔ frequency values of $CD3^+CD4^+CD40L^+$, TCM $CD40L^+$, and TCM/pTfh $CD40L^+$ T-cell subpopulations. Again, HIV variables clearly segregated from HC variables, and 2 clusters with opposite trends were generated: a main cluster with 30 proteins and matrix metalloprotease 10 segregating individually (Figure 5*E*). All the proteins of the main cluster demonstrated negative correlations (7 of 30 with $P < .05$) in the HIV group with the Ag-specific populations ($CD40L^+$) that, as described above, also failed their expansion at D28 conversely to HCs. Gene ontology analysis, exhibited in Figure 5*F*, reveals that the aforementioned molecules are mostly involved in the positive regulation of cytokine production, responses to cytokines, regulation of cell proliferation, and immune cell activation/proliferation or chemotaxis. In line with the humoral compartment, these results

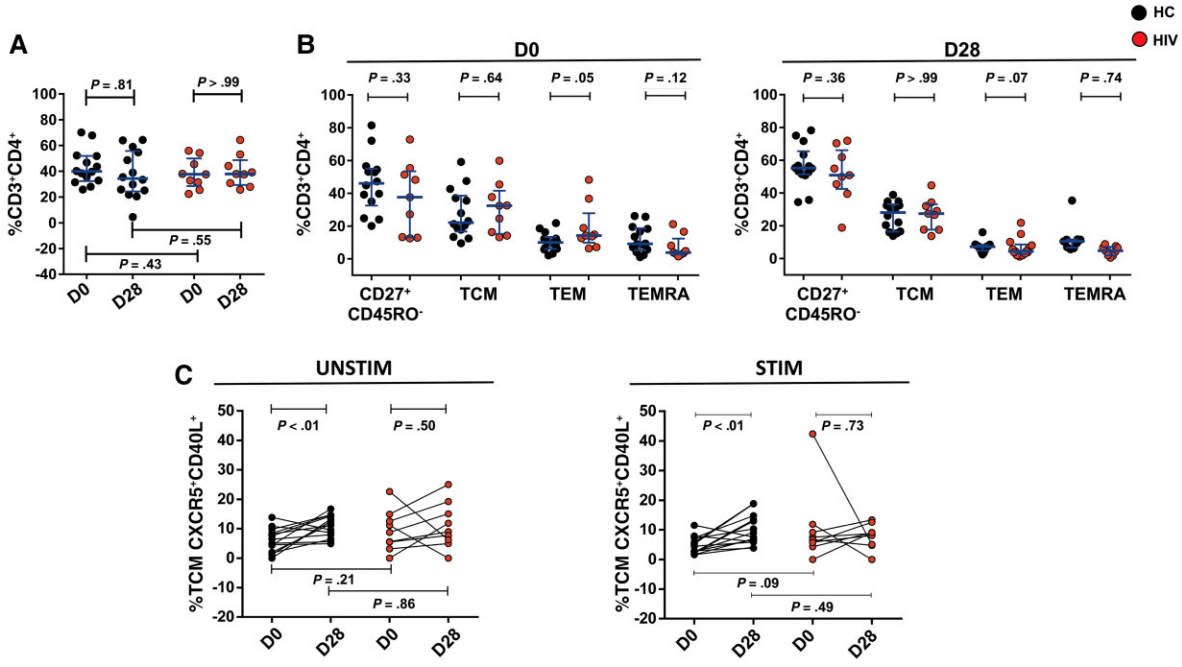

Figure 4. Human immunodeficiency virus (HIV)–infected patients demonstrate similar severe acute respiratory syndrome coronavirus 2 (SARS-CoV-2) messenger RNA BTN162b2-induced humoral but impaired cellular immunogenicity 4 weeks after the first dose (D28) of vaccination. Longitudinal analysis of total $CD3^+CD4^+$ T cells gated on live lymphocytes (*A*) and $CD3^+CD4^+$ T-cell subsets (*B*) in HIV-infected patients (red dots: n = 9) and healthy controls (HCs) (black dots: n = 14). Scatterplot graphs depict median with interquartile range. *C*, Frequencies of antigen-specific ($CD40L^+$) peripheral T-follicular helper cells, identified as TCM $CXCR5^+$, are shown for both the HIV (red dots: n = 9) and HC (black dots, n = 14) study groups at D0 and D28 in the absence (left panel) or presence (right panel) of 16 hours' in vitro stimulation with SARS-CoV-2 peptides. Wilcoxon signed-rank test and Mann-Whitney test were used to assess differences in the levels of each subpopulation between the time points and between the HC and HIV groups, respectively. Significance was set at $P < .05$. Abbreviations: HC, healthy controls; HIV, HIV-infected patients; STIM, stimulated; TCM, central memory T cells; TEM, effector memory T cells; TEMRA, terminally differentiated effector memory T cells; UNSTIM, unstimulated.

confirm the distinct profile that HIV^+ population displays at baseline in comparison to HCs. The entire sets of proteins either correlating with humoral or cellular variables are listed in Supplementary Figure 2*E* and 2*F*.

DISCUSSION

In the present study, we report for the first time distinct plasma proteomic, humoral, and cellular immune responses in a cohort of HIV^+ individuals immunized with Pfizer BNT162b2 mRNA vaccine. Our results build on a growing body of evidence in horizontally HIV-infected adults, and demonstrate how perinatally infected ART-treated patients with normal $CD4^+$ T-cell counts can mount robust specific immune responses to COVID-19 vaccine regardless of time of ART initiation [13, 14, 23]. Observational studies about vaccine responsiveness against different infectious agents, including SARS-CoV-2, in individuals with distinct immunity due to chronic conditions are fundamental in providing insights into further research to target vaccine intervention in these populations. Previous studies on the safety and immunogenicity of other vaccines in HIV^+ individuals represent the major existing backbone of knowledge to investigate COVID-19 vaccine responses in this group. Indeed, influenza vaccination studies conducted by our group and several other research groups in PLWH demonstrated that vaccine-induced specific responses were mostly related to $CD4^+$ T-cell counts plus a general ability of responder patients to better control HIV-related inflammation and aging. Accordingly, a recent study observed the inability of an HIV^+ subject with uncontrolled viremia and low $CD4^+$ T-cell count to develop an immune response after BNT162b2 vaccine [16], confirming the important role of $CD4^+$ T-cell count in mounting specific immune responses in mRNA vaccination strategies. In addition, younger individuals are more capable to effectively induce the production of SARS-CoV-2–specific Abs in comparison to elderly individuals [24]. In fact, all HIV study participants included in our cohort induced specific anti–SARS-CoV-2 responses upon vaccination as also observed by other researchers [10, 11]. The initial impairment within the HIV group in mounting comparable anti-trimeric S titers to HCs at D28 was subsequently overcome at D180 with HIV reaching younger HC Ab titers. pTfh cells are key among mononuclear cells in the production of Abs [25, 26]. Thus, our results

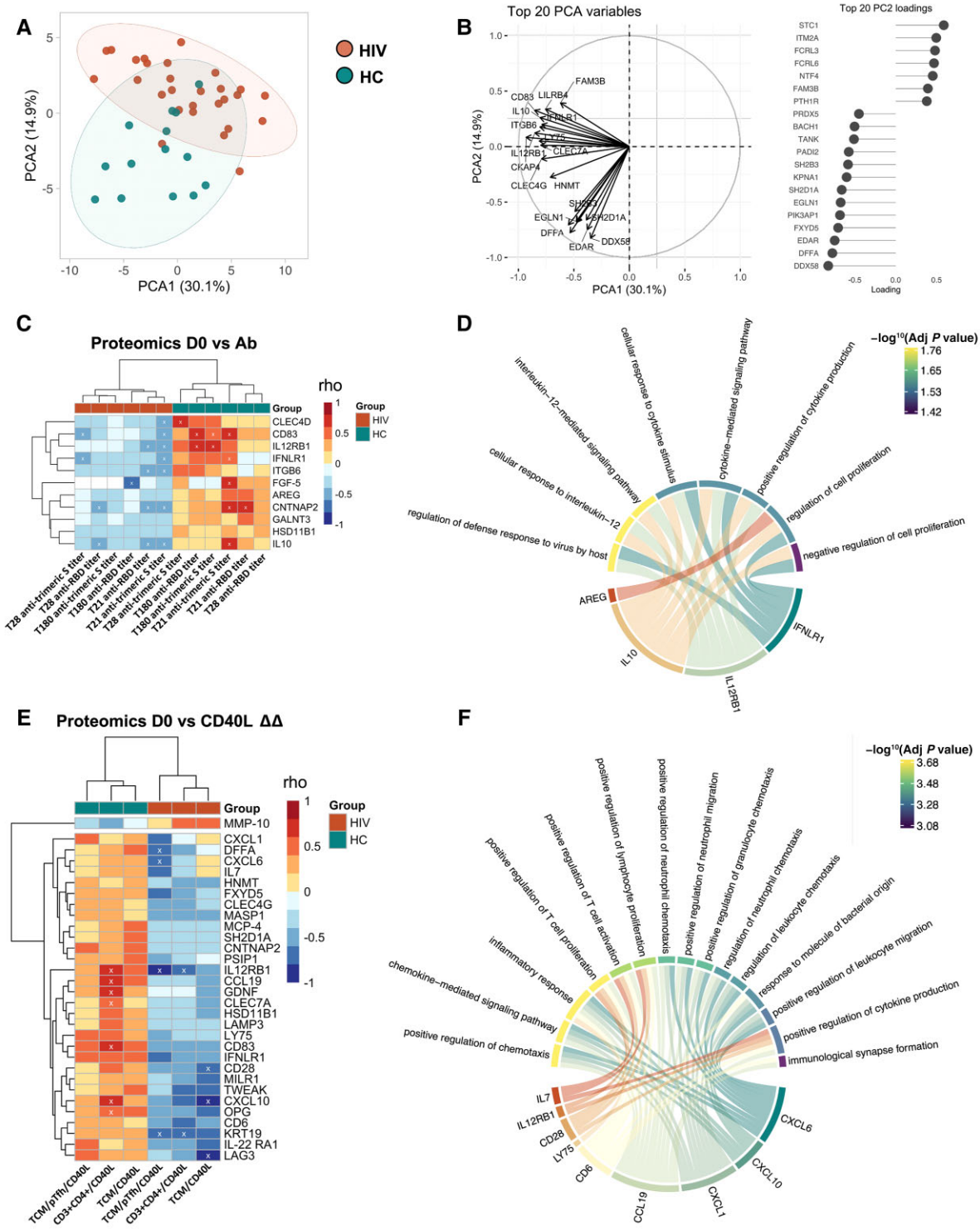

Figure 5. Human immunodeficiency virus (HIV)–infected patients demonstrate distinct correlation of baseline plasma proteomic profiles with BTN162b2 vaccine immunogenicity. Levels of 180 key protein biomarkers were characterized in study participant plasma samples via the high-multiplex Olink immunoassay by excluding proteins negatively or positively correlating with age (n = 45). *A*, Principal component analysis (PCA) of proteins' normalized protein expression values before vaccination (D0) in both the HIV (red dots, n = 28) and HC (green dots, n = 14) groups. *B*, The top 20 PC2 loading molecules are shown. Heatmap plots showing Spearman correlations (ρ) between plasma protein levels at D0 and anti-RBD and anti-trimeric S antibody titers at D21, D28, and D180 (*C*) or frequencies of antigen-specific ($CD40L^+$) $CD4^+$ T-cell subsets (*E*), expressed as delta-delta (ΔΔ) values, in the HIV (red) and HC (green) groups. To obtain the ΔΔ values, we calculated, for each $CD40L^+CD4^+$ T-cell population, the frequency difference between the stimulated and unstimulated samples (Δ) collected at D0 and D28, and then subtracted ΔD0 from ΔD28. Only correlations with an opposite trend in the HIV (red) and HC (green) groups are shown, with red indicating positive correlations and blue negative ones. The colored scale ranging from 1 and −1 indicates the ρ values. Crosses highlight significant correlations with $P < .05$. *D* and *F*, Circos plots depict gene ontology analyses, with colors related at the $\log_{10}$ adjusted *P* values. Significance was set at $P < .05$. Abbreviations: Ab, antibody; HC, healthy controls; HIV, HIV-infected patients; PCA, principal component analysis; pTfh, peripheral T follicular helper cells; RBD, receptor binding domain; TCM, central memory T cells.

suggested that the lower anti-trimeric S Abs titers at D28 could also be linked to $CD40L^+$ T-cell populations' inability to expand 7 days after booster dose. Indeed, future studies should verify whether this impairment is restored at follow-up time points also to a cellular level.

Overall, our observations suggest that for mRNA vaccines, neither the role of the early ART initiation, meant to restore the capabilities of the immune system, nor the immune senescence still described in PLWH despite an effective ART [27, 28], seem to have a significant impact on the immunogenicity of BNT162b2 vaccine.

Our results, although characterized by distinct features between the HC and HIV groups, suggested to us that the BNT162b2 mRNA vaccine can represent a good alternative to protect HIV^+ individuals. In fact, 3 study participants with a detectable VL at the time of enrollment did not present any increase in their VL after vaccination. Meanwhile, the 2 participants who experienced an increment in their VL at D28 resolved it within the 6 months of follow-up, suggesting, within the limits of our small study size, that the BNT162b2 vaccine does not induce uncontrollable HIV viremia as recently observed in wo studies conducted in horizontally infected adults (new ref.29 PMID: 35084386 DOI: 10.1097/QAD.0000000000003135; new ref.30 PMID: 35222357 DOI: 10.3389/fimmu.2021.820126).

The duality discussed so far in our cohort was more evident when we investigated the baseline host plasma proteome. In fact, the Olink panels we selected clearly segregated the study participants in 2 distinct cohorts with molecules noticeably interacting in opposite ways with either humoral or cellular data. These distinct profiles identified in the HC and HIV groups may inform future investigations regarding mRNA vaccines, to predict whether a vaccine may induce robust immunogenicity in a particular individual based on their baseline proteomic profiles. Indeed, the integration of systems vaccinology studies [29] has recently suggested that baseline signatures may be predictive of vaccine immunogenicity in HCs [30].

In conclusion, our study may suggest that perinatally HIV-infected patients, receiving ART and with normal $CD4^+$ T-cell counts, do not require a shortening of schedule set up for the additional dose of the COVID-19 vaccine. Additional factors such as older age, comorbidities, type of initial vaccine regimen, and durability of vaccine immunogenicity, affected by emerging viral variants such as Omicron, will also impact optimal guidance on the number of timing of potential booster doses in HIV-infected individuals. Overall, precision vaccinology will integrate clinical, immunologic, and systems biology data to inform the tailoring of vaccines to vulnerable populations for optimal safety and efficacy [31].

Supplementary Data

Supplementary materials are available at *Clinical Infectious Diseases* online. Consisting of data provided by the authors to benefit the reader, the posted materials are not copyedited and are the sole responsibility of the authors, so questions or comments should be addressed to the corresponding author.

Notes

Author Contributions. P. P. and P. R. conceived the study. C. P., E. M., G. R. P., N. C., C. M., D. A., L. C., A. R., E. C. M., C. C. T., S. B., and C. F. P. provided and/or analyzed clinical data. N. C., P. R., and P. P. acquired funding. E. M. and C. P. drafted the first version of the manuscript. All authors provided edits and comments to the final version.

Acknowledgments. The authors thank all patients and their families for participating in this study; the CONVERS "Evaluation of Covid-19 mRNA BNT162b2 (Comirnaty) vaccine immunogenicity in vulnerable populations" study nurses team; and Ilaria Pepponi, Jennifer Faudella, Giulia Neccia, and Patrizia Antimi for expert administrative assistance.

CONVERS Study Team. Lorenza Romani, MD; Sara Chiurchiù, MD; Andrea Finocchi, MD, PhD; Caterina Cancrini, MD, PhD; Laura Lancella, MD; Maia De Luca, MD, ; Chiara Rossetti, MD; Elisa Profeti, MD; and Enrica Franzese, MD.

Financial support. This work was supported in part by federal funds from the U.S. National Institutes of Health (NIH) through the Pediatric Adolescent Virus Elimination (PAVE) Martin Delaney Collaboratory (https://www.pave-collaboratory.org/), Project Number 1UM1 AI164566-01. The content of the manuscript is solely the responsibility of the authors and does not necessarily represent the official views of the National Institutes of Health. This work was also supported by Bambino Gesù Children's Hospital..

Supplement sponsorship. This supplement is sponsored by the *Precision Vaccines Program* of Boston Children's Hospital.

Potential conflicts of interest. O. L. is a named inventor on patents relating to anti-infective proteins, vaccines adjuvants, and human assay platforms that model vaccine immunogenicity in vitro. O.L.has also received consulting fees from Moody's analytics and funding from Boston Children's Hospital Department of Pediatrics and the Hospital's Chief Scientific Office. All other authors report no potential conflicts of interest.

All authors have submitted the ICMJE Form for Disclosure of Potential Conflicts of Interest. Conflicts that the editors consider relevant to the content of the manuscript have been disclosed.

References

1. Geretti AM, Stockdale AJ, Kelly SH, et al. Outcomes of coronavirus disease 2019 (COVID-19) related hospitalization among people with human immunodeficiency virus (HIV) in the ISARIC World Health Organization (WHO) Clinical Characterization Protocol (UK): a prospective observational study. Clin Infect Dis **2021**; 73:e2095–106.
2. Tesoriero JM, Swain CE, Pierce JL, et al. COVID-19 outcomes among persons living with or without diagnosed HIV infection in New York state. JAMA Netw Open **2021**; 4:e2037069.
3. Western Cape Department of Health in collaboration with the National Institute for Communicable Diseases South Africa. Risk factors for coronavirus disease 2019 (COVID-19) death in a population cohort study from the Western Cape Province, South Africa. Clin Infect Dis **2021**; 73: e2005–15.
4. Jedicke N, Stankov MV, Cossmann A, et al. Humoral immune response following prime and boost BNT162b2 vaccination in people living with HIV on antiretroviral therapy. HIV Med **2021**; 23:558–63.
5. Kanwugu ON, Adadi P. HIV/SARS-CoV-2 coinfection: a global perspective. J Med Virol **2021**; 93:726–32.
6. Sahin U, Muik A, Derhovanessian E, et al. COVID-19 vaccine BNT162b1 elicits human antibody and TH1 T cell responses. Nature **2020**; 586:594–9.
7. Polack FP, Thomas SJ, Kitchin N, et al. Safety and efficacy of the BNT162b2 mRNA Covid-19 vaccine. N Engl J Med **2020**; 383:2603–15.
8. Amodio D, Ruggiero A, Sgrulletti M, et al. Humoral and cellular response following vaccination with the BNT162b2 mRNA COVID-19 vaccine in patients affected by primary immunodeficiencies. Front Immunol **2021**; 12:727850.
9. Cotugno N, Pighi C, Morrocchi E, et al. Bnt162b2 mRNA COVID-19 vaccine in heart and lung transplanted young adults: is an alternative SARS-CoV-2 immune response surveillance needed? Transplantation **2022**; 106:e158–60.
10. Lacey CJ. HPV vaccination in HIV infection. Papillomavirus Res **2019**; 8:100174.

11. Kohler I, Kouyos R, Bianchi M, et al. The impact of vaccination on the breadth and magnitude of the antibody response to influenza A viruses in HIV-infected individuals. AIDS **2015**; 29:1803–10.
12. Tebas P, Frank I, Lewis M, et al. Poor immunogenicity of the H1N1 2009 vaccine in well controlled HIV-infected individuals. AIDS **2010**; 24:2187–92.
13. Woldemeskel BA, Karaba AH, Garliss CC, et al. The BNT162b2 mRNA vaccine elicits robust humoral and cellular immune responses in people living with human immunodeficiency virus (HIV). Clin Infect Dis **2022**; 74:1268–70.
14. Levy I, Wieder-Finesod A, Litchevsky V, et al. Immunogenicity and safety of the BNT162b2 mRNA COVID-19 vaccine in people living with HIV-1. Clin Microbiol Infect **2021**; 27:1851–5.
15. Heftdal LD, Knudsen AD, Hamm SR, et al. Humoral response to two doses of BNT162b2 vaccination in people with HIV. J Intern Med **2022**; 291:513–8.
16. Touizer E, Alrubayyi A, Rees-Spear C, et al. Failure to seroconvert after two doses of BNT162b2 SARS-CoV-2 vaccine in a patient with uncontrolled HIV. Lancet HIV **2021**; 8:e317–8.
17. Thomas SJ, Moreira ED, Jr, Kitchin N, et al. Safety and efficacy of the BNT162b2 mRNA Covid-19 vaccine through 6 months. N Engl J Med **2021**; 385:1761–73.
18. Sahin U, Muik A, Vogler I, et al. Bnt162b2 vaccine induces neutralizing antibodies and poly-specific T cells in humans. Nature **2021**; 595:572–7.
19. Zaffina S, Alteri C, Ruggiero A, et al. Induction of immune response after SARS-CoV-2 mRNA BNT162b2 vaccination in healthcare workers. J Virus Erad **2021**; 7:100046.
20. Lundberg M, Thorsen SB, Assarsson E, et al. Multiplexed homogeneous proximity ligation assays for high-throughput protein biomarker research in serological material. Mol Cell Proteomics **2011**; 10:M110.004978.
21. Cotugno N, Ruggiero A, Pascucci GR, et al. Virological and immunological features of SARS-COV-2–infected children with distinct symptomatology. Pediatr Allergy Immunol **2021**; 32:1833–42.
22. Chen EY, Tan CM, Kou Y, et al. Enrichr: interactive and collaborative HTML5 gene list enrichment analysis tool. BMC Bioinformat **2013**; 14:128.
23. Ruddy JA, Boyarsky BJ, Bailey JR, et al. Safety and antibody response to two-dose SARS-CoV-2 messenger RNA vaccination in persons with HIV. AIDS **2021**; 35: 2399–401.
24. Tut G, Lancaster T, Krutikov M, et al. Profile of humoral and cellular immune responses to single doses of BNT162b2 or ChAdOx1 nCoV-19 vaccines in residents and staff within residential care homes (VIVALDI): an observational study. Lancet Healthy Longev **2021**; 2:e544–e53.
25. Pallikkuth S, de Armas LR, Rinaldi S, et al. Dysfunctional peripheral T follicular helper cells dominate in people with impaired influenza vaccine responses: results from the FLORAH study. PLoS Biology **2019**; 17:e3000257.
26. Xing M, Feng Y, Yao J, et al. Induction of peripheral blood T follicular helper cells expressing ICOS correlates with antibody response to hepatitis B vaccination. J Med Virol **2020**; 92:62–70.
27. Zicari S, Sessa L, Cotugno N, et al. Immune activation, inflammation, and non-AIDS co-morbidities in HIV-infected patients under long-term ART. Viruses **2019**; 11:200.
28. Zhao J, Schank M, Wang L, et al. Mitochondrial functions are compromised in CD4 T cells from ART-controlled PLHIV. Front Immunol **2021**; 12:658420.
29. Diray-Arce J, Miller HER, Henrich E, et al. The immune signatures data resource: a compendium of systems vaccinology datasets. bioRxiv [Preprint]. Posted online 8 November 2021. doi:10.1101/2021.11.05.465336.
30. Fourati S, Tomalin LE, Mulè MP, et al. An innate immune activation state prior to vaccination predicts responsiveness to multiple vaccines. bioRxiv [Preprint]. Posted online 26 October 2021. doi:10.1101/2021.09.26.461847.
31. Soni D, Van Haren SD, Idoko OT, et al. Towards precision vaccines: lessons from the Second International Precision Vaccines Conference. Front Immunol **2020**; 11:590373.